AMERICAN SOCIETY FOR MICROBIOLOGY | Applied and Environmental Microbiology®

ENVIRONMENTAL MICROBIOLOGY

Differential Roles of Three Different Upper Pathway *meta* Ring Cleavage Product Hydrolases in the Degradation of Dibenzo-*p*-Dioxin and Dibenzofuran by *Sphingomonas wittichii* Strain RW1

Thamer Y. Mutter,[a,b] Gerben J. Zylstra[b]

[a]Department of Biology, College of Science, University of Anbar, Ramadi, Iraq
[b]Department of Biochemistry and Microbiology, School of Environmental and Biological Sciences, Rutgers University, New Brunswick, New Jersey, USA

ABSTRACT *Sphingomonas wittichii* RW1 grows on the two related compounds dibenzofuran (DBF) and dibenzo-*p*-dioxin (DXN) as the sole source of carbon. Previous work by others (P. V. Bunz, R. Falchetto, and A. M. Cook, Biodegradation 4:171–178, 1993, https://doi/org/10.1007/BF00695119) identified two upper pathway *meta* cleavage product hydrolases (DxnB1 and DxnB2) active on the DBF upper pathway metabolite 2-hydroxy-6-oxo-6-(2-hydroxyphenyl)-hexa-2,4-dienoate. We took a physiological approach to determine the role of these two enzymes in the degradation of DBF and DXN by RW1. Single knockouts of either plasmid-located *dxnB1* or chromosome-located *dxnB2* had no effect on RW1 growth on either DBF or DXN. However, a double-knockout strain lost the ability to grow on DBF but still grew normally on DXN, demonstrating that DxnB1 and DxnB2 are the only hydrolases involved in the DBF upper pathway. Using a transcriptomics-guided approach, we identified a constitutively expressed third hydrolase encoded by the chromosomally located SWIT0910 gene. Knockout of SWIT0910 resulted in a strain that no longer grows on DXN but still grows normally on DBF. Thus, the DxnB1 and DxnB2 hydrolases function in the DBF but not the DXN catabolic pathway, and the SWIT0190 hydrolase functions in the DXN but not the DBF catabolic pathway.

IMPORTANCE *S. wittichii* RW1 is one of only a few strains known to grow on DXN as the sole source of carbon. Much of the work deciphering the related RW1 DXN and DBF catabolic pathways has involved genome gazing, transcriptomics, proteomics, heterologous expression, and enzyme purification and characterization. Very little research has utilized physiological techniques to precisely dissect the genes and enzymes involved in DBF and DXN degradation. Previous work by others identified and extensively characterized two RW1 upper pathway hydrolases. Our present work demonstrates that these two enzymes are involved in DBF but not DXN degradation. In addition, our work identified a third constitutively expressed hydrolase that is involved in DXN but not DBF degradation. Combined with our previous work (T. Y. Mutter and G. J. Zylstra, Appl Environ Microbiol 87:e02464-20, 2021, https://doi.org/10.1128/AEM.02464-20), this means that the RW1 DXN upper pathway involves genes from three very different locations in the genome, including an initial plasmid-encoded dioxygenase and a ring cleavage enzyme and hydrolase encoded on opposite sides of the chromosome.

KEYWORDS dibenzo-*p*-dioxin, dibenzofuran, dioxin, *Sphingomonas*, biodegradation, degradation

Sphingomonas wittichii RW1 was isolated from the Elbe River in northern Germany for its ability to grow on both dibenzofuran (DBF) and dibenzo-*p*-dioxin (DXN) as the sole source of carbon and energy (1). RW1 metabolizes DBF and DXN by similar catabolic pathways initiated by an angular dioxygenase complex system that dihydroxylates one

Citation Mutter TY, Zylstra GJ. 2021. Differential roles of three different upper pathway *meta* ring cleavage product hydrolases in the degradation of dibenzo-*p*-dioxin and dibenzofuran by *Sphingomonas wittichii* strain RW1. Appl Environ Microbiol 87:e01067-21. https://doi.org/10.1128/AEM.01067-21.

Editor Rebecca E. Parales, University of California, Davis

Address correspondence to Gerben J. Zylstra, zylstra@sebs.rutgers.edu.

Received 30 May 2021
Accepted 24 August 2021
Accepted manuscript posted online 1 September 2021
Published 28 October 2021

of the aromatic rings forming a highly unstable intermediate that spontaneously decomposes to 2,2′,3-trihydroxydiphenyl (THD) and 2,2′,3-trihydroxydiphenyl ether (THDE), respectively (1, 2). A *meta* cleavage enzyme cleaves the dihydroxylated ring (3, 4) to form 2-hydroxy-6-oxo-6-(2-hydroxyphenyl)-hexa-2,4-dienoate (2OH-HOPDA) from THD and 2-hydroxy-6-oxo-6-(2-hydroxyphenoxy)-hexa-2,4-dienoate (2OH-O-HOPDA) from THDE. The alkene chain of the ring cleavage products is cleaved by a hydrolase (5, 6) forming salicylate (DBF pathway) or catechol (DXN pathway).

While aromatic hydroxylating dioxygenases are key enzymes in initiating the degradation of aromatic compounds, hydrolases are often a bottleneck in the degradation pathway (7–9). This is especially true for the degradation of compounds with more than one aromatic ring and for chlorinated compounds such as polychlorinated biphenyl (PCBs). Based on substrate specificity, bacterial hydrolases can be classified into three groups. Hydrolases belong to group I and II and are involved in bicyclic and monocyclic aromatic hydrocarbons, and those in group III are involved in heteroaromatics biodegradation (10). Due to their strict substrate specificity (11, 12), hydrolases limit the degradation of many aromatic hydrocarbons and their chlorinated substituents. An example is the BphD hydrolase from *Burkholderia xenovorans* strain LB400 that is a key enzyme in the biodegradation of many PCBs (13). Another important hydrolase is CarC from the carbazole-degrading *Pseudomonas resinovorans* CA10 that cleaves metabolites from both carbazole and DBF (14). One important example of the importance of hydrolases is a comparison of the *P. putida* F1 toluene degradation pathway and the *B. xenovorans* strain LB400 biphenyl degradation pathway. While the three initial enzymes in the F1 toluene pathway are capable of metabolizing biphenyl to HOPDA, the bottleneck for growth on biphenyl is the TodF hydrolase. Addition of the LB400 BphD hydrolase to F1 overcomes this bottleneck (8, 15). The catalytic mechanism of aromatic pathway hydrolases has been extensively examined (6, 11, 13, 16–24). The enzyme specificity is due to the conserved catalytic triad (nucleophile-acid-histidine) found in all alpha/beta superfamily *meta* cleavage product hydrolases where the nucleophile is always a serine (16, 19, 23).

Two isofunctional hydrolases (H1/DxnB1/SWIT4895 and H2/DxnB2/SWIT3055) have been purified from *S. wittichii* RW1 (5) grown on salicylate. Both of these enzymes hydrolyze 2-hydroxy-6-oxo-6-phenylhexa-2,4-dienoate [HOPDA] (biphenyl metabolite) and 2OH-HOPDA (DBF metabolite) to benzoate and salicylate, respectively. The two enzymes belong to the class III *meta* cleavage product hydrolases (6) but are monomeric (5), whereas other aromatic hydrolases are multimeric (11, 24, 25). While RW1 grows on both DBF and DXN, no information has been published on the activity of either of these two enzymes toward the DXN metabolite 2OH-O-HOPDA. The difference between 2OH-HOPDA (from DBF) and 2OH-O-HOPDA (from DXN) is the oxygen atom between the ring and the six carbon side chain in 2OH-O-HOPDA. SWIT3055/DxnB2 has been extensively studied and is known to hydrolytically cleave both C-C and C-O bonds (6, 20). Interestingly, *dxnB1* (SWIT4895) is localized to pSWIT02 in RW1 and is in the main DXN degradation locus (*dxnA1A2B1Cfdx3*) between the genes encoding the large and small subunits of the oxygenase component (*dxnA1A2*) and the ferredoxin component (*fdx3*) of the DBF/DXN dioxygenase. The *dxnB2* (SWIT3055) gene, on the other hand, is localized to the chromosome.

It is assumed that the DxnB1 and DxnB2 hydrolases are involved in the ability of RW1 to grow on both DXN and DBF. However, this is based on the activities of the purified enzymes and the constitutive nature of the cognate genes. By our count, the RW1 genome encodes 35 possible aromatic pathway hydrolases, and an examination of raw transcriptome sequencing (RNA-seq) data (26, 27) shows that three of these (SWIT0910, SWIT3055/*dxnB1*, and SWIT4895/*dxnB2*) are constitutively expressed. It is our hypothesis that all three of these constitutively expressed hydrolases are involved in RW1 DXN and/or DBF degradation. In the present work, we used a combination of gene knockout and physiological experiments to determine the role, if any, of each of these three hydrolases in RW1 DXN and DBF degradation.

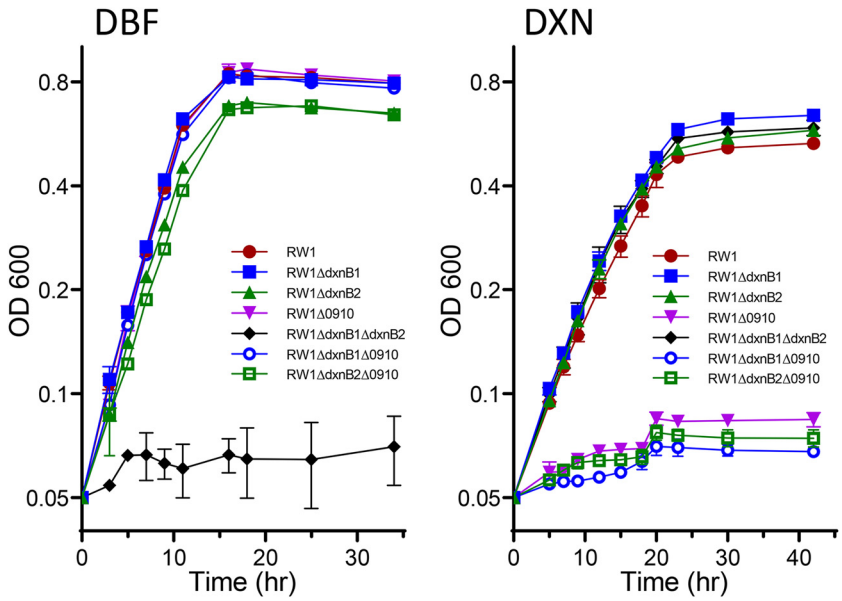

FIG 1 Growth of RW1, RW1ΔdxnB1, RW1ΔdxnB2, RW1Δ0910, RW1ΔdxnB1ΔdxnB2, RW1ΔdxnB1Δ0910, and RW1ΔdxnB2Δ0910 on dibenzofuran (DBF; left) and dibenzo-*p*-dioxin (DXN; right). Data are the averages of triplicates, and error bars indicate standard deviations.

RESULTS

DxnB1 (SWIT4895) and DxnB2 (SWIT3055) function in DBF degradation but not DXN degradation. Bunz et al. (5) previously isolated two isofunctional hydrolases active against HOPDA (biphenyl metabolite) and 2OH-HOPDA (DBF metabolite). Comparison of the N-terminal sequence of these two enzymes to the completed genome sequence (28) identified the genes as SWIT4895 (for H1/DxnB1) and SWIT3055 (for H2/DxnB2). In order to identify the role of each of these enzymes in DBF and DXN metabolism, we targeted these genes for knockout mutagenesis. As expected, RW1ΔdxnB1 and RW1ΔdxnB2 grew the same as the wild-type RW1 on DBF and DXN as the sole carbon source (Fig. 1). These data suggest that the enzymes are truly isofunctional under physiological conditions since both single knockouts grew normally. The double-knockout strain RW1ΔdxnB1ΔdxnB2 did not grow on DBF (Fig. 1), further demonstrating that the two hydrolases equally contribute to the third enzymatic step of DBF degradation and that no other RW1 hydrolase functions in this step of the pathway. Interestingly, the double-knockout RW1ΔdxnB1ΔdxnB2 grows on DXN (Fig. 1) at the same rate and extent as the wild-type RW1, showing that a third hydrolase must function in the DXN pathway and that this third hydrolase does not play a role in the DBF pathway.

Identification of a third hydrolase functional for DXN but not DBF degradation. By our count, the RW1 genome sequence contains genes encoding 35 potential aromatic compound pathway hydrolases (Fig. 2). There have been multiple transcriptomic and proteomic studies examining RW1 during growth on DXN, DBF, and related compounds (26, 27, 29–31). However, transcriptomic and proteomic studies typically report differences (ratios) in gene expression between growth on one substrate versus another. Since the RW1 DXN and DBF catabolic pathways are constitutively expressed (1), we examined the raw RNA-seq data from a transcriptomic study comparing DXN, DBF, and succinate grown RW1 (26). As expected, *dxnB1*/SWIT4895 and *dxnB2*/SWIT3055 are constitutively expressed with some slight variation (no more than 3 times) between the three growth substrates (Fig. 2). In addition, the SWIT0886 and SWIT0910 genes, encoding potential aromatic pathway hydrolases, were reported (26) to be constitutively expressed (Fig. 2). Raw SWIT0886 and SWIT0910 RNA-seq counts were about the same for growth on succinate and DXN but were down by approximately half for growth on

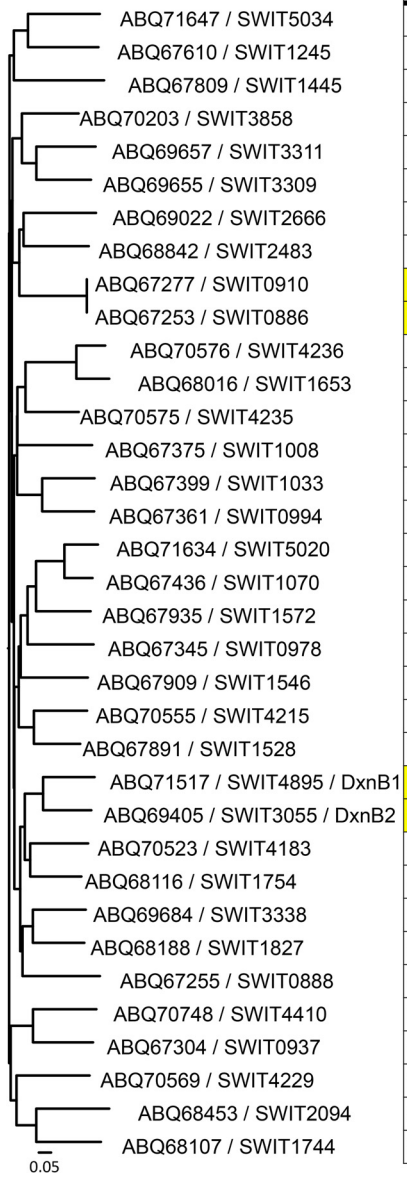

	RNA-Seq Counts		
Gene	SUC	DXN	DBF
SWIT 5034	162.99	151.4	143.54
SWIT 1245	25.27	23.45	25.26
SWIT 1445	3.17	4.3	3.44
SWIT 3858	3.77	1.28	1.65
SWIT 3311	0.99	1.29	0.79
SWIT 3309	14.31	9.96	20.32
SWIT 2666	17.95	18.76	17.2
SWIT 2483	4.38	3.52	8.37
SWIT 0910	2,376.23	2,626.57	1,254.69
SWIT 0886	1,030.20	1,157.20	552.09
SWIT 4236	1.21	2.09	0.35
SWIT 1653	3.98	4.8	3.29
SWIT 4235	2.37	2.4	1.6
SWIT 1008	0	0.37	0.74
SWIT 1033	6.92	5.92	4.41
SWIT 0994	30.11	98.33	32.89
SWIT 5020	6.58	6.75	9.28
SWIT 1070	3.62	8.35	4.22
SWIT 1572	0.99	1.29	0.93
SWIT 0978	9.18	83.4	4.26
SWIT 1546	3.37	7.95	3.09
SWIT 4215	3.39	3.75	3.32
SWIT 1528	2.6	1.95	2.51
SWIT 4895	5,295.23	4,085.90	5,934.15
SWIT 3055	7,624.89	10,553.19	3,783.40
SWIT 4183	1.61	2.78	1.56
SWIT 1754	3.79	4.73	4.37
SWIT 3338	2.79	8.88	2.94
SWIT 1827	2.79	3.85	2.2
SWIT 0888	6.18	9.34	9.58
SWIT 4410	22.98	23.34	28.47
SWIT 0937	8.76	7.03	9.9
SWIT 4229	4.97	6.49	4.88
SWIT 2094	6.37	2.97	3.72
SWIT 1744	3.22	4.26	3.49

FIG 2 Diversity of RW1 hydrolase enzymes with corresponding RNA-seq counts following growth on different substrates. In the amino acid sequence dendrogram, the ABQ number is the protein ID, and the SWIT number is the gene ID in the GenBank database. The gene designation for SWIT4895 is *dxnB1* and that for SWIT3055 is *dxnB2*. The RNA-seq numbers for each gene following growth on succinate (SUC), dibenzofuran (DBF), and dibenzo-*p*-dioxin (DXN) are extracted from Chai et al. (26) with GEO accession number GSE74831 and are the averages of multiple normalized replicates under each growth condition. Constitutive genes are highlighted in yellow.

DBF. Interestingly, SWIT0886 and SWIT0910 are nearly identical to each other, with 13 internal base pair differences out of 753 bases (changing only three amino acids) plus a nine-base "tail" on SWIT0910 (adding three amino acids to the end of the enzyme). Given that the two genes are 98.27% identical and that many RNA-seq software programs incorrectly assign RNA-seq reads to multiple gene copies, we reanalyzed the raw RNA-seq data in Chai et al. (26) for genes SWIT0886 and SWIT0910. RNA-seq reads with an exact (100%) match to SWIT0886 and/or SWIT0910 were binned into three categories, matching both SWIT0886 and SWIT0910, matching only SWIT0886, and matching only

TABLE 1 Reanalysis of raw RNA-seq data for the nearly identical genes SWIT0886 and SWIT0910 following growth of RW1 on DXN, DBF, and succinate

Growth substrate	SRA accession no.	No. of shared sequences	No. of sequences unique to SWIT0886	No. of sequences unique to SWIT0910
DXN	SRR2925812	1,827	0	266
	SRR2925813	2,459	5	349
	SRR2925814	1,511	3	206
DBF	SRR2925815	2,527	2	658
	SRR2925816	969	2	147
	SRR2925817	1,475	4	218
SUC[a]	SRR2925820	2,789	20	704
	SRR2925821	2,335	3	567

[a]SUC, succinate.

SWIT0910. The data (Table 1) show that SWIT0886 was not expressed on any of the three growth substrates (SWIT0886-only reads were 0.0% to 0.6% of the total reads) and that SWIT0910 was expressed on all three growth substrates (SWIT0910-only reads were 12% to 21% of the total reads). We therefore targeted SWIT0910 for gene knockout to examine its role in RW1 DXN and DBF metabolism. RW1Δ0910 grows the same as the wild-type strain RW1 on DBF (Fig. 1). This fact, coupled with the fact that RW1ΔDxnB1ΔDxnB2 does not grow on DBF, indicates that SWIT0910 plays no role in DBF degradation by RW1. Surprisingly, however, RW1Δ0910 does not grow on DXN (Fig. 1) and accumulates an orange-colored compound in the culture medium with a UV-visible (UV-Vis) spectrum consistent with 2OH-O-HOPDA. These data prove that SWIT0910 is the only RW1 hydrolase involved in growth of RW1 on DXN. The DBF pathway hydrolases DxnB1/SWIT4895, and DxnB2/SWIT3055 cannot take the place of SWIT0910 during growth on DXN even though they are constitutively expressed (Fig. 2). We also constructed the double-mutant strains RW1ΔDxnB1Δ0910 and RW1ΔDxnB2Δ0910 with the expected results: the double-knockout strains do not grow on DXN but do grow normally on DBF (Fig. 1).

Complementation. In order to prove that the growth effects described above are due to the specific gene knockout and not due to an effect on downstream genes, complementation experiments were performed. For the double-knockout RW1ΔdxnB1ΔdxnB2, addition of either plasmid pRK_dxnB1 or pRK_dxnB2 restored wild-type growth on DBF (Fig. 3), indicating that *lac* promoter-mediated expression of either of these two genes was sufficient to provide enough enzyme for complementation and that the knockout mutation only affected the *dxnB1* or *dxnB2* gene. For the knockout RW1Δ0910, complementation to wild-type growth on DXN (Fig. 3) was achieved not only with the pRK_0910 plasmid but also the pRK_0886 plasmid. As mentioned above, SWIT0886 and SWIT0910 are almost identical, but SWIT0886 is not expressed when RW1 is growing with succinate, DXN, or DBF as the carbon source. This means that both enzymes, despite their minor amino acid sequence differences, are capable of cleaving 2OH-O-HOPDA.

DISCUSSION

The work presented here demonstrates the value and culmination of a multifaceted approach to aromatic hydrocarbon degradation by a number of researchers over the last 29 years. *S. wittichii* RW1 was isolated in 1992 for the ability to grow on DBF and DXN (1). Two aromatic pathway hydrolases were purified (5), characterized in-depth (6, 22, 23), and their genes identified (28). The underlying physiology of RW1 DXN and DBF degradation has been probed using transcriptomic (26, 27, 31), proteomic (29, 30), and transposon insertion sequencing (Tn-seq) (32) methodologies. In the present work, we established that three different *meta* cleavage product hydrolases are involved in DXN and DBF degradation. Two of these hydrolases, DxnB1/SWIT4895 and DxnB2/SWIT3055, were previously isolated for the ability to cleave HOPDA (biphenyl pathway) and 2OH-HOPDA (DBF pathway). Surprisingly, neither of these two enzymes is capable

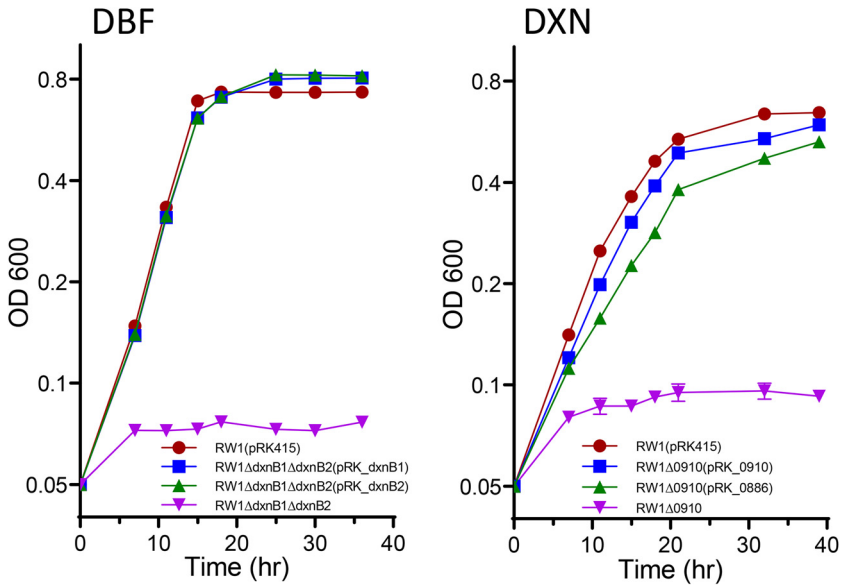

FIG 3 Complementation of the double *dxnB1* and *dxnB2* knockout strain by either cloned *dxnB1* or *dxnB2* on dibenzofuran (DBF; left) and complementation of the SWIT0910 knockout by either cloned SWIT0910 or SWIT0886 on dibenzo-*p*-dioxin (DXN; right).

of functioning in the RW1 DXN pathway, and both enzymes contribute equally to the RW1 DBF pathway. The single-knockouts RW1ΔDxnB1 and RW1ΔDxnB2 grow normally on DBF, and the double-knockout RW1ΔDxnB1ΔDxnB2 does not grow on DBF. All three knockout mutant strains grow on DXN. Using a combined genomic and transcriptomic approach, SWIT0910 was postulated to be the DXN pathway hydrolase, and a strain (RW1Δ0910) knocked out for this gene did not grow on DXN and grew normally on DBF. Based on these facts, we postulate that SWIT0910 has little or no activity toward the DBF metabolite 2OH-HOPDA and that DxnB1/SWIT4895 and DxnB2/SWIT3055 have little or no activity toward the DXN metabolite 2OH-O-HOPDA. Since the only difference between these two compounds is the oxygen linking the aromatic ring to the side chain, the oxygen must play a significant role in the ability (or inability) of the three hydrolases to cleave the compound. Based on this hypothesis, it is not surprising that the SWIT0910 hydrolase enzyme was not identified by Bunz et al. (5) since they did not screen using 2OH-O-HOPDA as the substrate. The three enzymes are sufficiently different from each other, with DxnB1 and DxnB2 sharing 44% amino acid identity over the full length of the protein and SWIT0910 showing less than 26% amino acid identity to DxnB1 and DxnB2 (Fig. 4). The DxnB2 enzyme has been extensively studied (6, 20–23) and the hydrolase catalytic triad (nucleophile-acid-histidine) identified as Ser105, Asp227, and His255. Interestingly, an alignment (Fig. 4) of the three enzymes DxnB1, DxnB2, SWIT0886, and SWIT0910 shows that Ser105 and Asp227 of DxnB2 are conserved in the other three enzymes but that the His255 is only conserved in DxnB1 but not in SWIT0886 and SWIT0910. Since the His255 is part of the catalytic triad in DxnB2, another amino acid must take its place in SWIT0886 and SWIT0910.

Sphingomonads are well-known for their ability to degrade a large number of compounds. This is correlated by the fact that their genomes encode many different degradative enzymes (28, 33) whose genes are not often organized in the typical operonic structure (34, 35). Soil organisms such as *S. wittichii* RW1 are constantly evolving to take advantage of changing environmental conditions and growth substrates (36, 37). Only a very few organisms are known to grow on DXN (1, 38–41). *S. wittichii* RW1 is the only one of these organisms that has been extensively studied. In contrast to DXN degradation, many strains have been isolated for the ability to degrade DBF, and many of these strains can partially metabolize DXN after growth (induction) on DBF. In RW1, the

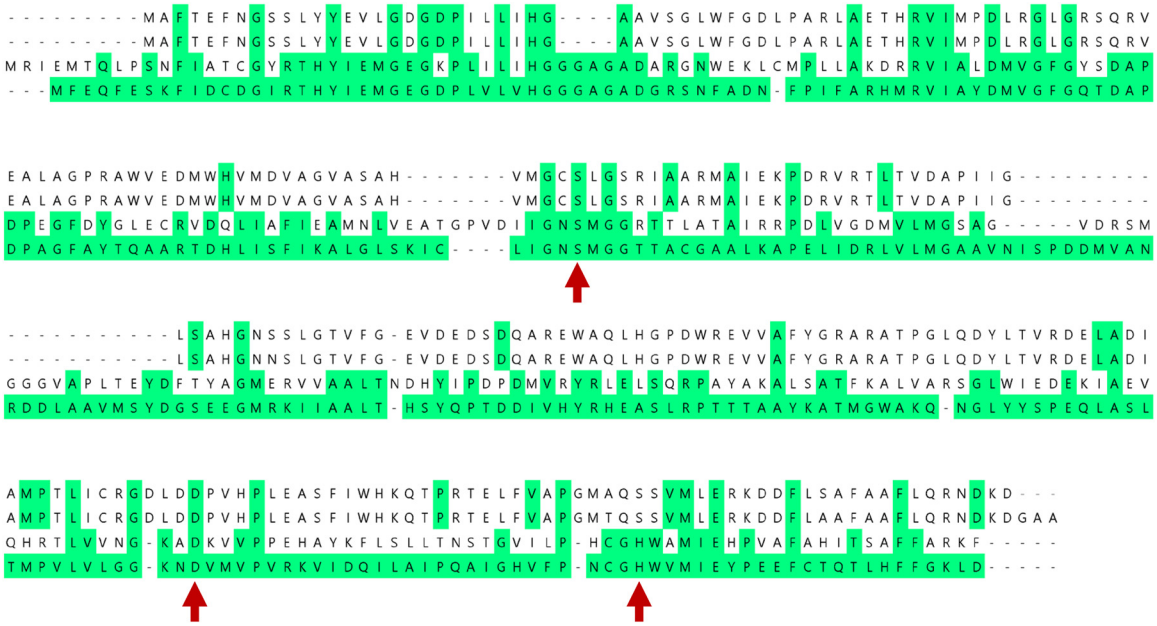

FIG 4 Alignment of SWIT0886, SWIT0910, DxnB1/SWIT4895, and DxnB2/SWIT3055 (top to bottom). Amino acid residues matching the best studied DxnB2/SWIT3055 are shaded in green. Three red arrows point to Ser105, Asp227, and His255 catalytic triad in DxnB2/SWIT3055, respectively.

genes encoding the upper pathway for DBF degradation are located in multiple locations on the plasmid pSWIT02. This plasmid is also found in other strains that can degrade DBF but not DXN (42). We previously showed (3) that DXN degradation absolutely depends on a THDE *meta* ring cleavage enzyme encoded by the chromosome. The DBF degradation pathway THD *meta* ring cleavage enzyme encoded by pSWIT02 does not function for THDE ring cleavage to allow RW1 growth on DXN. Now, in our current work, an analogous situation is discovered. There are two RW1 DBF degradation pathway 2OH-HOPDA hydrolases, one encoded by the chromosome and one encoded by pSWIT02 (Fig. 5). They are equally active in the catabolic pathway; deletion of one or the other does not affect RW1 growth on DBF. However, the DXN degradation pathway 2OH-O-HOPDA hydrolase is encoded by the RW1 chromosome and is absolutely required for growth (Fig. 5). Thus, the mystery of the complicated nature of RW1 DXN degradation is solved. The DXN catabolic pathway requires an initial ring hydroxylating dioxygenase encoded by pSWIT02. The remaining enzymes in the upper catabolic pathway, the THDE *meta* cleavage dioxygenase and the 2OH-O-HOPDA hydrolase, are encoded on opposite sides of the chromosome, over 2.3 megabases apart. Therefore, in order for nature to evolve an organism that grows on DXN, it was necessary to combine the pSWIT02 DBF degradative plasmid with the appropriate host-encoded genes.

MATERIALS AND METHODS

Bacterial strains, plasmids, media, and growth conditions. Strains and plasmids utilized in this study are listed in Table 2. Mineral salts basal medium (MSB) (43) was used as minimal medium and was supplemented with either L-phenylalanine (10 mM), DBF (3 mM), or DXN (3 mM) when needed. The insoluble DBF and DXN were added to MSB as described earlier (3). Amberlite IRA-400 chloride resin (Sigma-Aldrich, St. Louis, MO) was added at 2 mg/ml MSB broth when needed to prevent accumulation of 2OH-HOPDA or 2OH-O-HOPDA. RW1 and derivatives were grown aerobically at 30°C, and *Escherichia coli* strains were aerobically grown at 37°C. Tetracycline, kanamycin, gentamicin, and ampicillin were added to the medium when needed at 15, 50, 15, or 100 μg/ml, respectively. Growth curves were generated as described previously (3).

DNA techniques. Total genomic DNA was isolated with the Ultra Clean microbial kit (Qiagen, Germantown, MD), plasmids were isolated with the NucleoSpin plasmid kit (Macherey-Nagel, Bethlehem, PA), and DNA fragments isolated from gels with the GeneClean III kit (MP Biomedicals, Santa

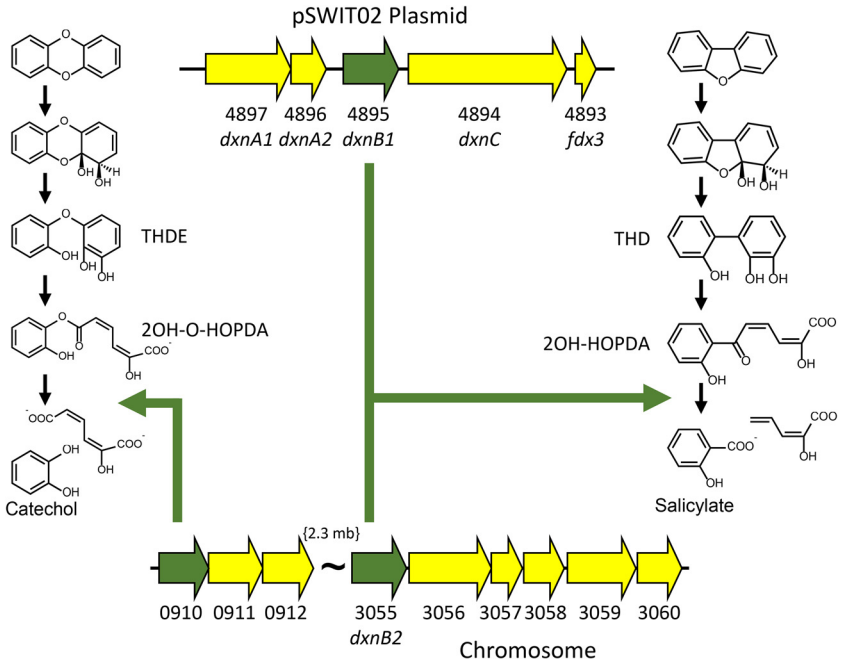

FIG 5 Metabolic map showing the role of the SWIT4895/DxnB1, SWIT0910, and SWIT3055/DxnB2 hydrolases in dibenzofuran and dibenzo-*p*-dioxin degradation by *S. wittichii* RW1. The SWIT4897/*dxnA1*, SWIT4896/*dxnA2*, SWIT4894/*dxnC*, and SWIT4893/*fdx3* genes encode the DXN/DBF oxygenase alpha and beta subunits, a TonB-like protein, and a dioxygenase ferredoxin, respectively. Genes SWIT0910, SWIT0911, and SWIT0912 encode a hydrolase and two nonidentical fumarylacetoacetate hydrolase family proteins. Genes SWIT3055 to SWIT3060 encode (in order) the DxnB2 hydrolase, oxygenase alpha and beta subunits, a putative maleylacetoacetate isomerase, a putative gentisate 1,2-dioxygenase, and a putative fumarylacetoacetate hydrolase. The chemical abbreviations are THD, 2,2′,3-trihydroxydiphenyl; THDE, 2,2′,3-trihydroxydiphenyl ether; 2OH-HOPDA, 2-hydroxy-6-oxo-6-(2-hydroxyphenyl)-hexa-2,4-dienoate; and 2OH-O-HOPDA, 2-hydroxy-6-oxo-6-(2-hydroxyphenoxy)-hexa-2,4-dienoate.

Ana, CA). Restriction digests, ligations, and PCRs were performed following standard protocols (New England Biolabs, Ipswich, MA). All cloned PCR products were sequenced to verify integrity of the final product. DNA sequencing was conducted by Genewiz (South Plainfield, NJ). PCR primers utilized in this study are listed in Table 3.

RNA-seq analysis. The RNA-seq raw data of Chai et al. (26, 27) were reanalyzed to accurately determine the sequence counts assigned to genes SWIT0886 and SWIT0910. The Magic-BLAST program (44) was used to query the Sequence Read Archive accession numbers SRR2925812 to SRR2925814 (DXN-grown RW1), SRR2925815 to SRR2925817 (DBF-grown RW1), and SRR2925820 to SRR2925821 (succinate-grown RW1) for exact (100%) matches to either SWIT0886 or SWIT0910. To calculate the unique sequence reads for each gene and those sequence reads in common, the matching sequence lists were compared with the online Venn diagram program (45) provided by Yves Van de Peer at the University of Ghent.

Construction of hydrolase knockout mutants and complementation. The three hydrolases were PCR amplified from RW1 gDNA using the Phusion high-fidelity PCR kit (NEB, Ipswich, MA). The *dxnB1* gene was PCR amplified with flanking regions of 0.60 kb upstream of the gene start codon and 0.47 kb downstream of the gene stop codon using the primers GGGGAATTCCGAAAGGCGCTCACTTCGAGGAC and GGGAATTCGAAGTTGCCGTGACACCG containing EcoRI restriction site on both ends. The resulting 1.92-kb DNA fragment was ligated into pGEM7Z (Promega, Madison, WI) after digestion with EcoRI to form pGEM7_dxnB1. The p34S-Km3 (46) kanamycin cassette was digested with SalI and ligated into similarly digested pGEM7_dxnB1 to form pGEM7_dxnB1-Km. The latter plasmid was digested with EcoRI and ligated into similarly digested pRK415 to make the final construct pRK_dxnB1KO-Km.

SWIT3055 (*dxnB2*) was PCR amplified with flanking regions of 0.54 kb upstream of the gene start codon and 0.42 kb downstream of the gene stop codon with the primers GGAAGCTTCTGGGTCACGCC TGCTTCG and GGTCTAGACCTAGCAGCTTGCCGTCATG containing HindIII and XbaI restriction sites, respectively. The resulting 1.8-kb fragment was TA cloned into pGEM-T Easy (Promega, Madison, WI) to form pGEMT_dxnB2. A gentamicin cassette was used to disrupt *dxnB2* in the unique BclI site after digestion of p34S-Gm (46) with BamHI (compatible end with BclI) to form pGEMT_dxnB2-Gm. The latter construct was digested with HindIII and XbaI and ligated into similarly digested pRK415 to form the final construct pRK_dxnB2KO-Gm.

The third hydrolase, SWIT0910, was PCR amplified with flanking regions of 0.70 kb upstream of the

TABLE 2 List of strains and plasmids used in this study

Strain or plasmid	Description	Source and/or reference
RW1	*Sphingomonas wittichii* RW1 wild-type strain	DSMZ (1)
RW1ΔdxnB1	RW1 with a kanamycin resistance cassette inserted into *dxnB1* (SWIT4895)	This study
RW1ΔdxnB2	RW1 with a gentamycin resistance cassette inserted into *dxnB2* (SWIT3055)	This study
RW1Δ0910	RW1 with a kanamycin resistance cassette inserted into SWIT0910	This study
RW1ΔdxnB1ΔdxnB2	RW1 with a kanamycin resistance cassette inserted into *dxnB1* (SWIT4895) and a gentamycin resistance cassette inserted into *dxnB2* (SWIT3055)	This study
RW1ΔdxnB1Δ0910	RW1 with a kanamycin resistance cassette inserted into *dxnB1* (SWIT4895) and a gentamycin resistance cassette inserted into SWIT0910	This study
RW1ΔdxnB2Δ0910	RW1 with a gentamycin resistance cassette inserted into *dxnB2* (SWIT3055) and a kanamycin resistance cassette inserted into SWIT0910	This study
pGEM7_dxnB1	pGEM7 containing *dxnB1* with flanking regions	This study
pGEM7_dxnB1-Km	pGEM7_dxnB1 with a kanamycin resistance cassette cloned into *dxnB1*	This study
pRK_dxnB1KO-Km	pRK415 with a kanamycin resistance cassette cloned into *dxnB1* for constructing the *dxnB1* knockout mutation	This study
pGEMT_dxnB2	pGEMT containing *dxnB2* with flanking regions	This study
pGEMT_dxnB2-Gm	pGEMT_dxnB2 with a gentamycin resistance cassette cloned into *dxnB2*	This study
pRK_dxnB2KO-Gm	pRK415 with a gentamycin resistance cassette cloned into *dxnB2* for constructing the *dxnB2* knockout mutation	This study
pET_0910	pET30a containing SWIT0910 with flanking regions	This study
pET_0910-Gm	pET_0910 with a gentamycin resistance cassette cloned into SWIT0910	This study
pET_0910-Km	pET_0910 with a kanamycin resistance cassette cloned into SWIT0910	This study
pRK_0910KO-Gm	pRK415 with a gentamycin resistance cassette cloned into SWIT0910 for constructing the SWIT0910 knockout mutation	This study
pRK_0910KO-Km	pRK415 with a kanamycin resistance cassette cloned into SWIT0910 for constructing the SWIT0910 knockout mutation	This study
pGEMT_0886	pGEMT containing SWIT0886	This study
pRK_0886	pRK415 containing SWIT0886 for complementation	This study
pCR_dxnB1	pCR2.1 containing *dxnB1*	This study
pCR_dxnB2	pCR2.1 containing *dxnB2*	This study
pCR_0910	pCR2.1 containing SWIT0910	This study
pRK_dxnB1	pRK415 containing *dxnB1* for complementation	This study
pRK_dxnB2	pRK415 containing *dxnB2* for complementation	This study
pRK_0910	pRK415 containing SWIT0910 for complementation	This study
pGEM-T Easy	TA cloning vector	Promega
pGEM7Z	Cloning vector	Promega
pET30a	Cloning vector	Sigma
pCR2.1	TOPO pCR2.1 vector	Thermo Fisher
pRK415	Unstable broad-host-range cloning vector	48
pRK2013	Helper plasmid for conjugation experiments	47
p34S-Km3	Source of the kanamycin resistance cassette	46, 49
p34S-Gm	Source of the gentamycin resistance cassette	46

gene start codon and 0.42 kb downstream of the gene stop codon with the primers GGAAGCTTGCAA CATCGTCCTGGTCG and GGAATTCGCAGGGCATAAGCGACGCAGTC containing HindIII and EcoRI restriction sites, respectively. The resulting 1.89-kb fragment was purified and digested with HindIII and EcoRI and ligated into similarly digested pET30a (Sigma, St. Louis, MO) to form pET_0910. A gentamicin or kanamycin cassette was used to disrupt SWIT0910 in the unique SalI site after digestion of pET_0910 and the antibiotic resistance cassette with SalI to form pET_0910-Gm or pET_0910-Km. The latter constructs were digested with HindIII and EcoRI and ligated into similarly digested pRK415 to form the final constructs pRK_0910KO-Gm or pRK_0910KO-Km.

The final knockout constructs in the unstable pRK415 vector were transferred into RW1 by triparental mating using the helper pRK2013 (47) with selection on MSB supplemented with phenylalanine and tetracycline. Knockouts resulting from homologous recombination were then selected by screening for loss of tetracycline resistance and retention of kanamycin or gentamicin resistance as described previously (3, 34).

SWIT0886 is nearly identical to SWIT0910. A 0.83-kb fragment of SWIT0886 was PCR amplified using the primers GGTTCTAGACCCAGGGCGACCGGCTATGTC and GAATTCGACGATGGCGGTCTTCATCGCG containing XbaI and EcoRI restriction sites (underlined), respectively. The PCR product was purified and cloned into the pGEM-T Easy vector to form pGEMT_0886. The gene was removed from pGEM_0886 with XbaI and EcoRI and ligated into similarly digested pRK415 to form pRK_0886. The final construct was transferred into RW1Δ0910 by triparental mating and transconjugants selected on MSB supplemented with phenylalanine and tetracycline.

Complementation of the mutations was performed by cloning the corresponding gene into pRK415

TABLE 3 List of PCR primers used in this study

Initial construct	PCR primer sequence (5′–3′)	PCR product
pGEM7Z_dxnB1	GGGGAATTCCGAAAGGCGCTCACTTCGAGGAC	*dxnB1* with flanking regions for knockout construction
	GGGAATTCGAAGTTGCCGTGACACCG	*dxnB1* with flanking regions for knockout construction
pGEMT_dxnB2	GGAAGCTTCTGGGTCACGCCTGCTTCG	*dxnB2* with flanking regions for knockout construction
	GGTCTAGACCTAGCAGCTTGCCGTCATG	*dxnB2* with flanking regions for knockout construction
pET_0910	GGAAGCTTGCAACATCGTCCTGGTCG	SWIT0910 with flanking regions for knockout construction
	GGAATTCGCAGGGCATAAGCGACGCAGTC	SWIT0910 with flanking regions for knockout construction
pGEMT_0886	GGTTCTAGACCCAGGGCGACCGGCTATGTC	SWIT0886 for complementation
	GAATTCGACGATGGCGGTCTTCATCGCG	SWIT0886 for complementation
pCR_dxnB1	GGGAATTCGGGGAATCGTGAGGATAGAAATGACCCAGC	*dxnB1* for complementation
	CCCAAGCTTGCATGCTAGAATTTCCGAGCG	*dxnB1* for complementation
pCR_dxnB2	GTCGACGACGGCATTGCCGGTCGGTG	*dxnB2* for complementation
	AAGCTTCGGCCATCGATCAATCCAGC	*dxnB2* for complementation
pCR_0910	GAATTCGGAGGACGGATTGGGGATC	SWIT0910 for complementation
	AAGCTTATCGCTGGCGAGGGGAGGAT	SWIT0910 for complementation

under *lac* promoter expression. Gene cassettes for the three hydrolase genes were constructed by cloning appropriate PCR fragments into the TOPO pCR2.1 vector (Thermo Fisher, Waltham, MA). Forward primers incorporated an EcoRI or a SalI site and reverse primers incorporated a HindIII site. A 0.87-kb SWIT4895/*dxnB1* PCR fragment was amplified using the primers GGGAATTCGGGGAATCGTGAGGAT AGAAATGACCCAGC and CCCAAGCTTGCATGCTAGAATTTCCGAGCG, a 0.82-kb PCR fragment containing SWIT0910 was amplified using the primers GAATTCGGAGGACGGATTGGGGATCG and AAGCTTATCGCT GGCGAGGGGAGGAT, and a 0.89-kb PCR fragment containing SWIT3055/*dxnB2* was amplified using the primers GTCGACGACGGCATTGCCGGTCGGTG and AAGCTTCGGCCATCGATCAATCCAGC. The three hydrolases were digested with XbaI and KpnI from pCR_dxnB1, pCR_dxnB2, and pCR_0910, gel purified, and ligated into similarly digested pRK415 to form pRK_dxnB1, pRK_dxnB2, and pRK_0910, respectively. The resulting constructs were transferred into the mutant strains by triparental mating with selection on MSB supplemented with phenylalanine and tetracycline.

ACKNOWLEDGMENTS

T.Y.M. gratefully acknowledges the support of the Higher Committee for Education Development (HCED) in Iraq for fellowship support. G.J.Z. acknowledges support from NIEHS grant P42-ES004911 under the Superfund Research Program.

REFERENCES

1. Wittich RM, Wilkes H, Sinnwell V, Francke W, Fortnagel P. 1992. Metabolism of dibenzo-*p*-dioxin by *Sphingomonas* sp. strain RW1. Appl Environ Microbiol 58:1005–1010. https://doi.org/10.1128/aem.58.3.1005-1010.1992.
2. Bunz PV, Cook AM. 1993. Dibenzofuran 4,4a-dioxygenase from *Sphingomonas* sp. strain RW1: angular dioxygenation by a three-component enzyme system. J Bacteriol 175:6467–6475. https://doi.org/10.1128/jb.175.20.6467-6475.1993.
3. Mutter TY, Zylstra GJ. 2021. Separate upper pathway ring cleavage dioxygenases are required for growth of *Sphingomonas wittichii* strain RW1 on dibenzofuran and dibenzo-*p*-dioxin. Appl Environ Microbiol 87:e02464-20. https://doi.org/10.1128/AEM.02464-20.
4. Happe B, Eltis LD, Poth H, Hedderich R, Timmis KN. 1993. Characterization of 2,2',3-trihydroxybiphenyl dioxygenase, an extradiol dioxygenase from the dibenzofuran- and dibenzo-*p*-dioxin-degrading bacterium *Sphingomonas* sp. strain RW1. J Bacteriol 175:7313–7320. https://doi.org/10.1128/jb.175.22.7313-7320.1993.
5. Bunz PV, Falchetto R, Cook AM. 1993. Purification of two isofunctional hydrolases (EC 3.7.1.8) in the degradative pathway for dibenzofuran in *Sphingomonas* sp. strain RW1. Biodegradation 4:171–178. https://doi.org/10.1007/BF00695119.
6. Seah SY, Ke J, Denis G, Horsman GP, Fortin PD, Whiting CJ, Eltis LD. 2007. Characterization of a C-C bond hydrolase from *Sphingomonas wittichii* RW1 with novel specificities towards polychlorinated biphenyl metabolites. J Bacteriol 189:4038–4045. https://doi.org/10.1128/JB.01950-06.
7. Furukawa K, Tomizuka N, Kamibayashi A. 1979. Effect of chlorine substitution on the bacterial metabolism of various polychlorinated biphenyls. Appl Environ Microbiol 38:301–310. https://doi.org/10.1128/aem.38.2.301-310.1979.
8. Furukawa K, Hirose J, Suyama A, Zaiki T, Hayashida S. 1993. Gene components responsible for discrete substrate specificity in the metabolism of biphenyl (*bph* operon) and toluene (*tod* operon). J Bacteriol 175:5224–5232. https://doi.org/10.1128/jb.175.16.5224-5232.1993.
9. Hirose J, Suyama A, Hayashida S, Furukawa K. 1994. Construction of hybrid biphenyl (*bph*) and toluene (*tod*) genes for functional analysis of aromatic ring dioxygenases. Gene 138:27–33. https://doi.org/10.1016/0378-1119(94)90779-x.
10. Alcaide M, Tornes J, Stogios PJ, Xu X, Gertler C, Di Leo R, Bargiela R, Lafraya A, Guazzaroni ME, Lopez-Cortes N, Chernikova TN, Golyshina OV, Nechitaylo TY, Plumeier I, Pieper DH, Yakimov MM, Savchenko A, Golyshin PN, Ferrer M. 2013. Single residues dictate the co-evolution of dual esterases: MCP hydrolases from the alpha/beta hydrolase family. Biochem J 454:157–166. https://doi.org/10.1042/BJ20130552.
11. Seah SY, Terracina G, Bolin JT, Riebel P, Snieckus V, Eltis LD. 1998. Purification and preliminary characterization of a serine hydrolase involved in the microbial degradation of polychlorinated biphenyls. J Biol Chem 273:22943–22949. https://doi.org/10.1074/jbc.273.36.22943.
12. Seeger M, Timmis KN, Hofer B. 1995. Conversion of chlorobiphenyls into phenylhexadienoates and benzoates by the enzymes of the upper pathway for polychlorobiphenyl degradation encoded by the *bph* locus of *Pseudomonas* sp. strain LB400. Appl Environ Microbiol 61:2654–2658. https://doi.org/10.1128/aem.61.7.2654-2658.1995.
13. Seah SY, Labbe G, Nerdinger S, Johnson MR, Snieckus V, Eltis LD. 2000. Identification of a serine hydrolase as a key determinant in the microbial degradation of polychlorinated biphenyls. J Biol Chem 275:15701–15708. https://doi.org/10.1074/jbc.275.21.15701.
14. Nojiri H, Taira H, Iwata K, Morii K, Nam JW, Yoshida T, Habe H, Nakamura S, Shimizu K, Yamane H, Omori T. 2003. Purification and characterization

of *meta*-cleavage compound hydrolase from a carbazole degrader *Pseudomonas resinovorans* strain CA10. Biosci Biotechnol Biochem 67:36–45. https://doi.org/10.1271/bbb.67.36.
15. Zylstra GJ, Chauhan S, Gibson DT. Degradation of chlorinated biphenyls by *Escherichia coli* containing cloned genes of the *Pseudomonas putida* F1 toluene catabolic pathway, p 290–302. *In* Oppelt ET (ed), Proceedings of the sixteenth annual hazardous waste research symposium: remedial action, treatment, and disposal of hazardous waste, Cincinnati, OH, 3 to 5 April 1990. EPA/600/9 90/037.
16. Habe H, Morii K, Fushinobu S, Nam JW, Ayabe Y, Yoshida T, Wakagi T, Yamane H, Nojiri H, Omori T. 2003. Crystal structure of a histidine-tagged serine hydrolase involved in the carbazole degradation (CarC enzyme). Biochem Biophys Res Commun 303:631–639. https://doi.org/10.1016/s0006-291x(03)00375-9.
17. Seah SY, Labbe G, Kaschabek SR, Reifenrath F, Reineke W, Eltis LD. 2001. Comparative specificities of two evolutionarily divergent hydrolases involved in microbial degradation of polychlorinated biphenyls. J Bacteriol 183:1511–1516. https://doi.org/10.1128/JB.183.5.1511-1516.2001.
18. Horsman GP, Ke J, Dai S, Seah SY, Bolin JT, Eltis LD. 2006. Kinetic and structural insight into the mechanism of BphD, a C-C bond hydrolase from the biphenyl degradation pathway. Biochemistry 45:11071–11086. https://doi.org/10.1021/bi0611098.
19. Fushinobu S, Jun SY, Hidaka M, Nojiri H, Yamane H, Shoun H, Omori T, Wakagi T. 2005. A series of crystal structures of a *meta*-cleavage product hydrolase from *Pseudomonas fluorescens* IP01 (CumD) complexed with various cleavage products. Biosci Biotechnol Biochem 69:491–498. https://doi.org/10.1271/bbb.69.491.
20. Ruzzini AC, Horsman GP, Eltis LD. 2012. The catalytic serine of *meta*-cleavage product hydrolases is activated differently for C-O bond cleavage than for C-C bond cleavage. Biochemistry 51:5831–5840. https://doi.org/10.1021/bi300663r.
21. Ruzzini AC, Ghosh S, Horsman GP, Foster LJ, Bolin JT, Eltis LD. 2012. Identification of an acyl-enzyme intermediate in a *meta*-cleavage product hydrolase reveals the versatility of the catalytic triad. J Am Chem Soc 134:4615–4624. https://doi.org/10.1021/ja208544g.
22. Ruzzini AC, Bhowmik S, Yam KC, Ghosh S, Bolin JT, Eltis LD. 2013. The lid domain of the MCP hydrolase DxnB2 contributes to the reactivity toward recalcitrant PCB metabolites. Biochemistry 52:5685–5695. https://doi.org/10.1021/bi400774m.
23. Ruzzini AC, Bhowmik S, Ghosh S, Yam KC, Bolin JT, Eltis LD. 2013. A substrate-assisted mechanism of nucleophile activation in a Ser-His-Asp containing C-C bond hydrolase. Biochemistry 52:7428–7438. https://doi.org/10.1021/bi401156a.
24. Lam WWY, Bugg TDH. 1997. Purification, characterization, and stereochemical analysis of a C-C hydrolase: 2-hydroxy-6-keto-nona-2,4-diene-1,9-dioic acid 5,6-hydrolase. Biochemistry 36:12242–12251. https://doi.org/10.1021/bi971115r.
25. Otwinowski Z, Minor W. 1997. Processing of X-ray diffraction data collected in oscillation mode. Macromolecular Crystallography, Pt A 276:307–326. https://doi.org/10.1016/S0076-6879(97)76066-X.
26. Chai B, Tsoi TV, Iwai S, Liu C, Fish JA, Gu C, Johnson TA, Zylstra G, Teppen BJ, Li H, Hashsham SA, Boyd SA, Cole JR, Tiedje JM. 2016. *Sphingomonas wittichii* strain RW1 genome-wide gene expression shifts in response to dioxins and clay. PLoS One 11:e0157008. https://doi.org/10.1371/journal.pone.0157008.
27. Chai B, Tsoi T, Sallach JB, Liu C, Landgraf J, Bezdek M, Zylstra G, Li H, Johnston CT, Teppen BJ, Cole JR, Boyd SA, Tiedje JM. 2020. Bioavailability of clay-adsorbed dioxin to *Sphingomonas wittichii* RW1 and its associated genome-wide shifts in gene expression. Sci Total Environ 712:135525. https://doi.org/10.1016/j.scitotenv.2019.135525.
28. Miller TR, Delcher AL, Salzberg SL, Saunders E, Detter JC, Halden RU. 2010. Genome sequence of the dioxin-mineralizing bacterium *Sphingomonas wittichii* RW1. J Bacteriol 192:6101–6102. https://doi.org/10.1128/JB.01030-10.
29. Colquhoun DR, Hartmann EM, Halden RU. 2012. Proteomic profiling of the dioxin-degrading bacterium *Sphingomonas wittichii* RW1. J Biomed Biotechnol 2012:408690. https://doi.org/10.1155/2012/408690.
30. Hartmann EM, Armengaud J. 2014. Shotgun proteomics suggests involvement of additional enzymes in dioxin degradation by *Sphingomonas wittichii* RW1. Environ Microbiol 16:162–176. https://doi.org/10.1111/1462-2920.12264.
31. Coronado E, Roggo C, Johnson DR, van der Meer JR. 2012. Genome-wide analysis of salicylate and dibenzofuran metabolism in *Sphingomonas wittichii* RW1. Front Microbiol 3:300. https://doi.org/10.3389/fmicb.2012.00300.
32. Roggo C, Coronado E, Moreno-Forero SK, Harshman K, Weber J, van der Meer JR. 2013. Genome-wide transposon insertion scanning of environmental survival functions in the polycyclic aromatic hydrocarbon degrading bacterium *Sphingomonas wittichii* RW1. Environ Microbiol 15:2681–2695. https://doi.org/10.1111/1462-2920.12125.
33. Zhao Q, Hu H, Wang W, Peng H, Zhang X. 2015. Genome sequence of *Sphingobium yanoikuyae* B1, a polycyclic aromatic hydrocarbon-degrading strain. Genome Announc 3:e01522-14. https://doi.org/10.1128/genomeA.01522-14.
34. Kim E, Zylstra GJ. 1999. Functional analysis of genes involved in biphenyl, naphthalene, phenanthrene, and *m*-xylene degradation by *Sphingomonas yanoikuyae* B1. J Ind Microbiol Biotechnol 23:294–302. https://doi.org/10.1038/sj.jim.2900724.
35. Armengaud J, Happe B, Timmis KN. 1998. Genetic analysis of dioxin dioxygenase of *Sphingomonas* sp. strain RW1: catabolic genes dispersed on the genome. J Bacteriol 180:3954–3966. https://doi.org/10.1128/JB.180.15.3954-3966.1998.
36. Koskella B, Vos M. 2015. Adaptation in natural microbial populations. Annu Rev Ecol Evol Syst 46:503–522. https://doi.org/10.1146/annurev-ecolsys-112414-054458.
37. Chase AB, Weihe C, Martiny JBH. 2021. Adaptive differentiation and rapid evolution of a soil bacterium along a climate gradient. Proc Natl Acad Sci U S A 118:e2101254118. https://doi.org/10.1073/pnas.2101254118.
38. Hong HB, Nam IH, Murugesan K, Kim YM, Chang YS. 2004. Biodegradation of dibenzo-*p*-dioxin, dibenzofuran, and chlorodibenzo-*p*-dioxins by *Pseudomonas veronii* PH-03. Biodegradation 15:303–313. https://doi.org/10.1023/b:biod.0000042185.04905.0d.
39. Kimura N, Urushigawa Y. 2001. Metabolism of dibenzo-*p*-dioxin and chlorinated dibenzo-*p*-dioxin by a Gram-positive bacterium, *Rhodococcus opacus* SAO101. J Biosci Bioeng 92:138–143. https://doi.org/10.1263/jbb.92.138.
40. Hiraishi A. 2003. Biodiversity of dioxin-degrading microorganisms and potential utilization in bioremediation. Microb Environ 18:105–125. https://doi.org/10.1264/jsme2.18.105.
41. Saibu S, Adebusoye SA, Oyetibo GO. 2020. Aerobic bacterial transformation and biodegradation of dioxins: a review. Bioresour Bioprocess 7:7. https://doi.org/10.1186/s40643-020-0294-0.
42. Stolz A. 2014. Degradative plasmids from sphingomonads. FEMS Microbiol Lett 350:9–19. https://doi.org/10.1111/1574-6968.12283.
43. Stanier RY, Palleroni NJ, Doudoroff M. 1966. The aerobic pseudomonads: a taxonomic study. J Gen Microbiol 43:159–271. https://doi.org/10.1099/00221287-43-2-159.
44. Boratyn GM, Thierry-Mieg J, Thierry-Mieg D, Busby B, Madden TL. 2019. Magic-BLAST, an accurate RNA-seq aligner for long and short reads. BMC Bioinformatics 20:405. https://doi.org/10.1186/s12859-019-2996-x.
45. Van de Peer Y. Calculate and draw custom Venn diagrams. http://bioinformatics.psb.ugent.be/webtools/Venn/. Accessed 30 May 2021.
46. Dennis JJ, Zylstra GJ. 1998. Plasposons: modular self-cloning minitransposon derivatives for rapid genetic analysis of Gram-negative bacterial genomes. Appl Environ Microbiol 64:2710–2715. https://doi.org/10.1128/AEM.64.7.2710-2715.1998.
47. Figurski DH, Helinski DR. 1979. Replication of an origin-containing derivative of plasmid RK2 dependent on a plasmid function provided in *trans*. Proc Natl Acad Sci U S A 76:1648–1652. https://doi.org/10.1073/pnas.76.4.1648.
48. Keen NT, Tamaki S, Kobayashi D, Trollinger D. 1988. Improved broad-host-range plasmids for DNA cloning in Gram-negative bacteria. Gene 70:191–197. https://doi.org/10.1016/0378-1119(88)90117-5.
49. Dennis JJ, Zylstra GJ. 1998. Improved antibiotic-resistance cassettes through restriction site elimination using Pfu DNA polymerase PCR. Biotechniques 25:772–774. https://doi.org/10.2144/98255bm04.